MODELING COMPLEXITY OF PHYSIOLOGICAL TIME SERIES *IN-SILICO*

Jesse Berwald, Tomáš Gedeon
Department of Mathematics, Montana State University, Bozeman, Montana, U.S.A.

Konstantin Mischaikow
Department of Mathematics and BioMaPS Institute, Rutgers University, Piscataway, New Jersey, U.S.A.

Keywords: Physiological time series, Complexity, Neural networks.

Abstract: A free-running physiological system produces time series with complexity which has been correlated to the robustness and health of the system. The essential tool to study the link between the structure of the system and the complexity of the series it produces is a mathematical model that is capable of reproducing the statistical signatures of a physiological time series. We construct a model based on the neural structure of the hippocampus that reproduces *detrended fluctuations* and *multiscale entropy* complexity signatures of physiological time series. We study the dependence of these signatures on the length of the series and on the initial data.

1 INTRODUCTION

Measuring an output of a physiological system provides a window into its complex multi-scale dynamics. The measurements are often spread over time and many techniques of time series analysis have been used to gain an insight into the underlying physiology. Some of the most intriguing observations indicate that the complexity of the time series produced by a free-running physiological system, as measured by Detrended Fluctuation Analysis (DFA), Multiscale Entropy (MSE) and other methods, is correlated to the robustness and health of the physiological system. More precisely, analysis of time series gathered from the measurement of cardiac inter-beat intervals, oscillations of red blood cells, gait analysis, and other patterns observed in living organisms (Goldberger, 2006; Goldberger et al., 2000; Costa et al., 2002; Costa et al., 2005; Peng et al., 1994; Peng et al., 2007) suggests that healthy systems produce complex time series, while compromised systems produce either very simple periodic signals, or completely random signals.

The potential diagnostic and therapeutic consequences of this hypothesis demand studies that go beyond passive analysis of existing data. What is needed is a model which reproduces observed characteristics of physiological signals and thence can be actively tested. Ideally, such a model would be based on our knowledge of a complex system. However, it has proved challenging to construct a dynamical system-based model that reproduces the statistical characteristics of physiological time series. The only successful attempt was a discrete map with added noise (Peng et al., 2007) which partially reproduced some of these characteristics.

The central aim of our work is to construct a deterministic FitzHugh-Nagumo-based neural network model which exhibits the complex signatures measured by DFA and MSE metrics in physiological signals. We study the dependence of these metrics on the length of the computed time series and initial conditions used. Note that this issue has relevance to the analysis of experimental time series. One tacitly assumes that the analyzed series represents the steady response of the system, which does not depend on initial data, or the time when the measurements started. The longer the time series, the more time the system has for the initial data effect to "average out". While these assumptions are satisfied if the deterministic system is ergodic and stationary, we can test them directly in our model.

The model consists of a network of five excitatory cells and five inhibitory cells. The structure and dynamics of the network are based on the work of Terman (Terman et al., 2008) modeling the structure of

Berwald J., Gedeon T. and Mischaikow K. (2010).
MODELING COMPLEXITY OF PHYSIOLOGICAL TIME SERIES IN-SILICO.
In *Proceedings of the Third International Conference on Bio-inspired Systems and Signal Processing*, pages 61-67
DOI: 10.5220/0002710300610067

the hippocampus. Analyzing the time series of averages from the excitatory cells' voltage potential, we show that it matches the DFA and MSE measurements of complexity for free-running physiological systems across a range of time scales. These results do not depend on the initial conditions used. Furthermore, we show that the range of complex behavior grows when we increase the length of the time series from 15,000 to 100,000 (in arbitrary units), but does not grow further, when we extend the length to 400,000.

This indicates that the system has a certain capacity for complexity which does not depend on initial conditions, and which is recovered from data of finite length.

2 NEURAL NETWORK MODEL

We create a bipartite graph $G = \langle V_E, V_I, A \rangle$, where V_E consists of excitatory nodes, or cells, V_I consists of inhibitory cells, and A is the set of directed edges which consists of the following types of connections:

$$e_j \to i_k, \quad i_k \to e_j, \text{ and } i_k \to i_{k'},\ k \neq k',$$

where e denotes an excitatory cell and i denotes an inhibitory cell; $j \in \{1,\ldots,n\}$ and $k,k' \in \{1,\ldots,m\}$,and $n = |V_E|$, $m = |V_I|$. Excitatory cells do not connect to other excitatory cells in order to avoid the blow-up of the solutions due to runaway positive feedback. The subgraph V_I is complete. We construct the remaining connections randomly by selecting the $e_j \to i_k$ and $i_k \to e_j$ edges with probability $\rho = (\ln N)/N$, where $N = n+m$. Figure 1 shows a sample neural network. Edges are weighted by a maximal conductance constant which depends on the type of connection. We represent these weights by g_{IE}, g_{EI}, $g_{II} \in (0,1)$, where the subscripts E and I denote excitatory and inhibitory edges, respectively, and g_{xy} specifies the weight for the directed edge $x \to y$.

2.1 FitzHugh-Nagumo Equations

The following system of coupled differential equations describes the behavior of each cell in the graph defined above (Terman et al., 2008). All units are arbitrary.

Inhibitory cells:

$$\begin{aligned}\frac{dv}{dt} &= v - \frac{v^3}{3} - w - g_{II}(v - v_I)\left(\sum s_k\right) \\ &\quad - g_{EI}(v - v_E)\left(\sum s_j\right) + K_I(t) \\ \frac{dw}{dt} &= \varepsilon(v - bw + c)\end{aligned}$$

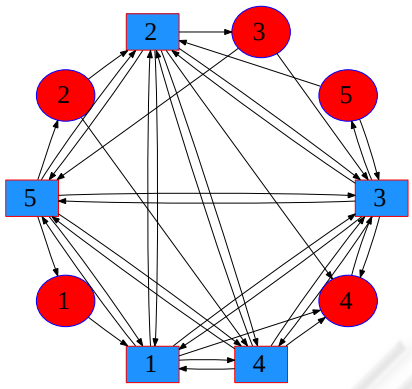

Figure 1: A neural network with ten cells. Inhibitory cells (I) are represented by blue squares, excitatory cells (E) by red ellipses. The subgraph of I cells is completely connected. $E \to I$ and $I \to E$ edges are created with probability $\frac{\ln N}{N}$. $E \to E$ edges are not allowed.

$$\begin{aligned}\frac{ds}{dt} &= \alpha_I(1-s)h(x,\theta_x) - \beta_I s \\ \frac{dx}{dt} &= \varepsilon[\alpha_x(1-x)h(v,\theta_I) - \beta_x x]. \qquad (1)\end{aligned}$$

Excitatory cells:

$$\begin{aligned}\frac{dv}{dt} &= v - \frac{v^3}{3} - w - g_{IE}(v - v_I)\left(\sum s_k\right) + K_E(t) \\ \frac{dw}{dt} &= \varepsilon(v - bw + c) \\ \frac{ds}{dt} &= \alpha(1-s)h(v,\theta) - \beta s, \qquad (2)\end{aligned}$$

In general, the coupling variable s represents the fraction of open synaptic channels. The coupling sums, $\sum s_k$ and $\sum s_j$, are limited to those cells connecting to the given cell; s_k is the input from an inhibitory cell, s_j is the input from an excitatory cell.

A direct synapse is one in which the postsynaptic receivers are themselves ion channels. In equations (2) an excitatory cell is modeled with a direct synapse. The function h is a steep sigmoidal curve allowing for a very rapid, but still continuous, activation of the synaptic processes. Once the voltage potential v crosses θ the synapse activates (h turns on) and an impulse travels to connected cells.

An indirect synapse, where the postsynaptic receivers are not ion channels, is modeled by adding the delay variable x. All inhibitory synapses in our model are indirect. The activation of the synaptic variable s relies on x, not v as in a direct synapse. In the bottom equation of (1), v must first reach the threshold θ_I in order to activate x. After this delay, x goes on to activate s.

Each cell is assigned a unique $\varepsilon \ll 1$. If the cell oscillates when disconnected from the other cells, ε

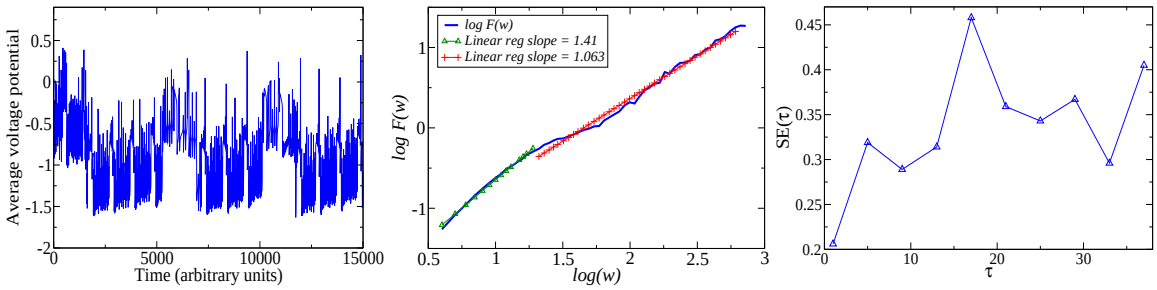

(a) (b) (c)

Figure 2: (a) Time series for a simulation run for 15000 "seconds" (units are arbitrary). (b) The DFA curve exhibits two trends: at short scales we observe autocorrelation effects due to deterministic ODE solver, at longer scales we find a scaling exponent of $\beta = 1.063$, similar to physiological systems, though over a shorter range. The relatively short time series produces more variability in the higher window sizes since the number of data points used to calculate the DFA becomes small. (c) Sample entropy $SE(\tau) = SE(m, \delta, N, \tau)$ is calculated for $\tau = 1, 5, \ldots, 37$, $m = 7$, and $\delta = 0.2$. The length, N, of the coarse-grained time series depends on τ. The MSE curve has an average of $\overline{SE} = 0.35$. The variance of $Var(SE) = 0.003$ is larger than in longer simulations. As in (b), this greater variability is due to the relatively small number of data points in the original time series.

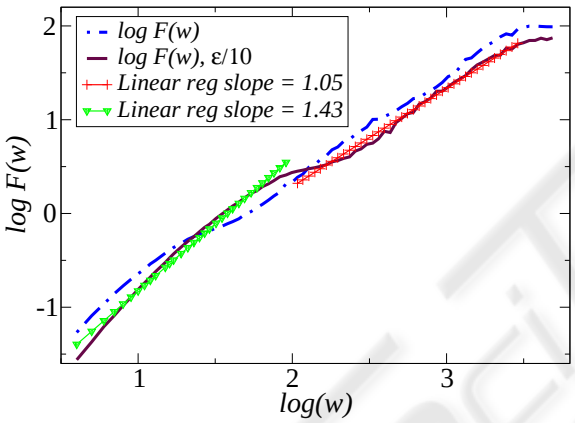

Figure 3: DFA curve from an initial ε distribution (solid blue), and the DFA curve obtained by dividing each ε by 10 (dashed purple).

is inversely proportional to the period of this oscillation. The constants v_E and v_I are reversal potentials for excitatory and inhibitory cells, respectively. The maximal conductance constants g_{IE}, g_{EI}, g_{II} weight a cell's input by multiplying the coupling terms.

The parameters $\alpha, \alpha_I, \alpha_x, \beta, \beta_I, \beta_x \in \mathbb{R}$ are rates at which the synaptic variables, s and x, turn on and off. The linear recovery term is specified by the parameters $b, c \in \mathbb{R}$. And the K_E and K_I terms represent external input to the system. In order for cells to enter an excitatory state a small amount of input must be applied to the system. For simplicity we use constant input. The complete set of parameters used is listed in the Appendix.

2.2 *In-Silico* Neural Network

An *in-silico* neural network, $\mathcal{N}$ is constructed from the following constituent pieces. The structure and behavior of the network is specified in a graph G composed of cells whose behavior is described by (1) and (2). A parameter set P contains fixed parameters for the FitzHugh-Nagumo equations. Thus, $\langle G, P \rangle$ generate a unique neural network $\mathcal{N}$ used for simulations.

3 TIME SERIES ANALYSIS

Solving the above system of ODE's with an adaptive step solver results in a set of solutions for each cell. The voltage potentials, $v_j(t)$, from all excitatory cells are averaged at each time step to give a time series $g(t)$. The analysis techniques require equally spaced time steps. Since an adaptive step algorithm returns irregularly spaced time steps we construct a new time series by partitioning the time axis into *bins* and averaging over these bins, giving a time series composed of the values

$$\bar{g}(n) = \frac{1}{\kappa T} \sum_{i=n(\kappa T)}^{(n+1)(\kappa T)} g(i), \tag{3}$$

where $n = 0, 1, \ldots, L = \lfloor \frac{M}{\kappa T} \rfloor$, M is the length of $g(t)$, and κ is chosen so that each bin contains a minimum number of points. Note that a small tail of the original time series must be discarded. We apply the following techniques to series $\bar{g}(n)$.

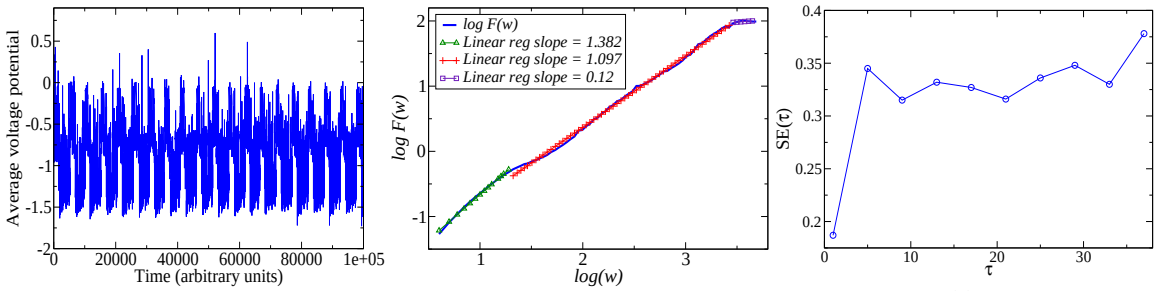

(a) (b) (c)

Figure 4: (a) Time series from simulating $\mathcal{N}$ for 100000. (b) The region of physiological complexity for the DFA curve extends from $w = 10^{1.3}$ to $w = 10^{3.5}$. For windows larger than $10^{3.5}$ we observe a new, flat trend indicating that the time series generated by $\mathcal{N}$ is devoid of long range correlations for these larger windows. (c) The MSE curve is relatively constant over a large number of scales indicating physiological complexity in the time series. The average sample entropy for $\tau \geq 5$ is $\overline{SE} = 0.34$, with a variance of $Var(SE) = 0.0007$.

3.1 Detrended Fluctuation Analysis

Detrended fluctuation analysis is a statistical method developed to determine long term trends in time series (Peng et al., 1994; Peng et al., 1995). Given a time series of length N, it is first integrated at each point to give a function $y(t) = \int_0^t g(s)\,ds$. The time axis is then partitioned into windows of length w. Next, a linear regression line, $y_w(t)$, is fit to the integrated curve for each window. The root-mean-square of the *detrended* curve $y(t) - y_w(t)$ is calculated, giving the detrended fluctuation value for a window size w:

$$F(w) = \sqrt{\frac{1}{N}\sum_{k=0}^{N}(y(t) - y_w(t))^2},$$

where y_w is understood to be the linear regression to y defined piecewise over each window of length w. F is computed for a wide range of window sizes and typically increases monotonically. Power law scaling exists in the time series when a log-log plot produces a linear relationship.

3.2 Multiscale Entropy

Multiscale entropy (Costa et al., 2005; Costa et al., 2002) simulates the sequence of refinements in the definition of Kolmogorov-Sinai (KS) entropy (Katok and Hasselblatt, 1997). In the case of MSE, though, we are interested in the evolution of the entropy across these refinements, and not their limit. Suppose we obtain a time series $g(t)$ by taking measurements of an experiment. This gives a sequence of data points $\{g(0), g(1), \ldots, g(N)\}$. MSE simulates the situation where we perform the identical experiment with less time accuracy. A time series for this situation is constructed through *coarse graining*, or partitioning the time axis of the original series into blocks of size $\tau \in \mathbb{N}$ and averaging the data over these windows. Thus, each coarse grained time series is composed of the points

$$g_\tau(n) = \frac{1}{\tau}\sum_{k=n\tau}^{(n+1)\tau} g(k),$$

where $n = 0, 1, \ldots, L = \lfloor N/\tau \rfloor$.

The entropy of this new time series $\{g_\tau(0), g_\tau(1), \ldots, g_\tau(L)\}$ is estimated using *sample entropy* (Richman and Moorman, 2000). Sample entropy views a time series as a sequence of random variables and measures the creation of information by computing the correlation between delay vectors of length m and $m+1$.

In order to define sample entropy, fix τ and set $g_\tau(i) = x_i$. Given m, let $u_m(i) = \{x_i, x_{i+1}, \ldots, x_{i+m}\}$ be a delay vector of length m, and define the number of vectors close to $u_m(i)$ as $n_i^m(\delta) = \#\{x_m(j) : d(x_m(i), x_m(j)) < \delta\}$ where $\delta > 0$ is some tolerance and $d = \max_{k=0,1,\ldots,m}\{|\, x_m(i+k) - x_m(j+k)\,|\}$. There are $N(m) = L - m$ full length vectors $u_m(j)$, excluding the possibility of self matches. The probability of finding the vector $u_m(j)$ within a distance δ of $u_m(i)$ is

$$C_i^m(\delta) = \frac{n_i^m(\delta)}{N(m)}.$$

For the parameter m the probability that any two vectors are within δ of each other is

$$C^m(\delta) = \frac{1}{N(m)}\sum_{i=0}^{N(m)} C_i^m(\delta)$$

The above *correlation integral* is used to define the sample entropy for the delay m, tolerance δ, and time series length L as

$$SE(m, \delta, L) = -\ln\frac{C^{m+1}}{C^m}.$$

C^{m+1}/C^m is commonly thought of as the information gained as the trajectory moves from time $m\tau$ to $(m+1)\tau$. A larger difference between C^m and C^{m+1} results in more information, i.e., a higher value of SE. For a fixed value of m the graph of the sample entropy over a range of τ's provides a measure of the amount of long range correlation in the time series. A relatively constant amount of entropy across many values of τ signifies correlations amongst data points over multiple time scales. For instance, $1/f$ noise which is highly correlated across time scales yields a constant MSE curve. In contrast, white noise is monotonically decreasing since it possesses no long range correlations.

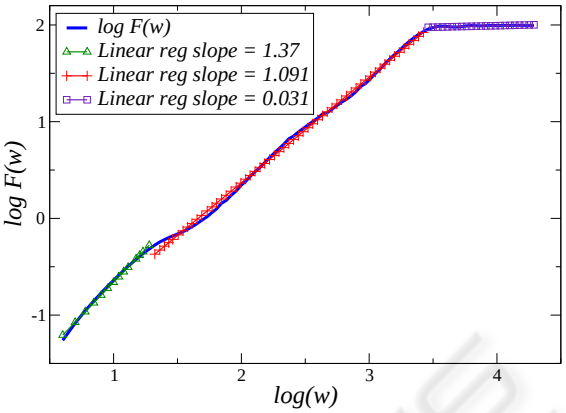

Figure 5: The DFA curve after simulating $\mathcal{N}$ for $N = 400000$. The region of complexity remains unchanged from that seen in Figure 4(b). This implies that $\mathcal{N}$ has an inherent limit for generating long range correlations.

4 RESULTS

Consider an *in-silico* neural network $\mathcal{N}$ as defined in Section 2.2. We construct the time series of voltage potentials $\bar{g}(n)$ by choosing a set of initial conditions and solving the system of differential equations over the time interval $[0, N]$, then performing the binning procedure described in (3). The units of time are arbitrary.

Figure 2 shows the time series, DFA curve, and MSE curve for a simulation of $\mathcal{N}$ run for $N = 15000$. In Figure 2(b), the scaling exponent $\beta = 1.063$ over the range of window sizes $w = 10^{1.3}$ to $w = 10^{2.7}$. Thus, running $\mathcal{N}$ for a relatively short simulation produces power law scaling similar to a physiological system over the range $(1.3, 2.7)$ for the total length of range 1.4 . This range of scales where $\beta \approx 1$ is shorter than that typically seen in biological systems, where the range typically has length greater than 3. The DFA curve extracted from our simulations has three distinct regions. In the first region, where $w < 10^{1.3}$, the linear regression deviates from the power law $\beta \approx 1$ due to autocorrelation effects on short scales, which are caused by the deterministic ODE solver. These effects dominate at scales much smaller than the highest frequency cellular oscillations, which can be estimated from the largest ε. Figure 3 illustrates this effect; we compare the DFA curve in Figure 4(b) to the curve obtained after dividing by 10 all of the ε's used in generating Figure 4(b). The deterministic portion extends to higher scales because the highest oscillation frequency decreased by a factor of ten. This also illustrates the importance of the choice of ε's on the DFA curve. In order to avoid these deterministic effects we focus (for the original set of ε's listed in the Appendix) on power law scaling in the second region, where $w > 10^{1.3}$.

In Figure 2(b) we see that $\mathcal{N}$ produces physiologically complex behavior in the region $w > 10^{1.3}$, which ends at $w = 10^{2.7}$. By increasing the length of the time series (Figure 4(b)) the second region extends past $w = 10^{2.7}$ to $w = 10^{3.5}$ showing that $\mathcal{N}$ continues to introduce complexity into the time series past the scale limits imposed by the short simulation in Figure 2. The second region terminates in Figure 4(b) at $w = 10^{3.5}$, where a third region with no long range correlation begins. Extending the length of the simulation to $N = 400000$ yields the DFA curve in Figure 5, where this third region extends to larger window sizes. Clearly the extension of the time series fails to find longer range correlations in the time series. We conclude that the system $\mathcal{N}$ has an upper limit $w = 10^{3.5}$ on the length of long range correlations it can generate.

The longer time series yields an MSE curve that is relatively constant, mimicking the behavior observed in simulation of $1/f$-noise as well as free-running physiological systems. It maintains an entropy level nearly identical to the MSE curve in Figure 2(c). Indeed, the average entropies for $\tau \geq 5$ are $\overline{SE} = 0.34$ and $\overline{SE} = 0.35$, respectively. The MSE curve in Figure 2(c) derived from the shorter time series suffers larger variations due to coarse graining effects on the relatively low number of data points in the original series. Nevertheless, as the comparison of the averages shows the MSE and sample entropy measures for shorter simulations are consistent with the results from longer simulations, and still provide good insight into the complexity of the network.

Furthermore, the behavior of $\mathcal{N}$ does not depend on initial conditions as we confirm by choosing random initial conditions for excitatory cells uniformly in the interval $(-5, 5)$. To illustrate, we present a typical case in which we alter the initial condition of

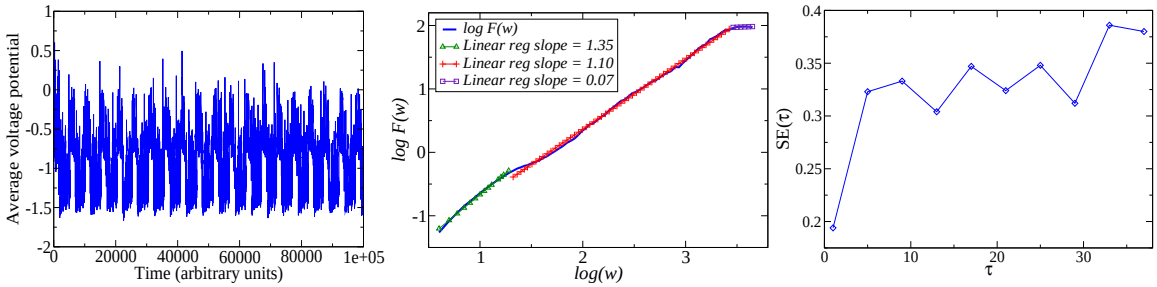

(a) (b) (c)

Figure 6: (a) Time series resulting from choosing a different initial condition for the excitatory cell e_1 compared to Figure 4 and simulating $\mathcal{N}$ for $N = 100000$. (b) The DFA curve exhibits a nearly identical scaling exponent $\beta = 1.10$ over the middle region as the curve in Figure 4(b). Long range correlations are unaffected by initial conditions. (c) The MSE curve has slightly different values at the various scales, but the average entropy for $\tau \geq 5$ is $\overline{SE} = 0.34$ which is identical to that produced by $\mathcal{N}$ in Figure 4. The variance $Var(SE) = 0.0003$ is similar as well.

one excitatory cell, e_1. Figure 6 shows the time series and related analysis obtained by using a random initial condition. Comparison of the time series in Figure 6(a) to the one in Figure 4(a) shows minor differences. Importantly, the scaling exponent for the DFA curve in Figure 6(b) differs from that in Figure 4(b) by less than 0.01. The mean value of the entropy for both MSE curves is $\overline{SE} = 0.34$. Figure 7 shows a comparison of the MSE curves from Figures 4(c) and 6(c). In the MSE curve resulting from the random initial condition each $SE(\tau)$ value is slightly perturbed from the original, but the general behavior of the MSE curve remains unchanged. Thus, long range correlations and entropy are independent of the initial condition used for simulating $\mathcal{N}$.

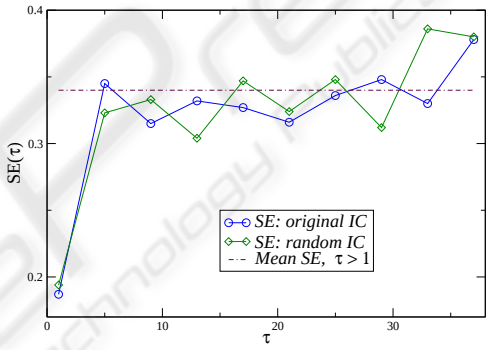

Figure 7: Comparison of MSE curves for the initial condition used in the simulation in Figures 2 and 4 and a randomly chosen initial condition for the excitatory cell e_1. For $\tau \geq 5$, $\overline{SE}(\tau) = 0.34$ for both curves. The original initial condition is -0.5; the randomly initial condition is 0.7957.

5 CONCLUSIONS

The link between the complexity of a time series produced by a free-running physiological system and that system's robustness and health has potential applications in the diagnosis and treatment of physiological ailments. To make the leap to clinical applications, this observed correlation must be put on a firmer footing by understanding more precisely the causal link between the dynamics and structure of the system on one hand, and the time series structure on the other. Mathematical models will play a decisive role in this process, since they allow for direct testing of this connection.

It has proven quite challenging to construct such models. We report here on a successful attempt, where we show that a randomly connected small network of FitzHugh-Nagumo neurons can reproduce detrended fluctuations and multiscale entropy observed in physiological time series. In analyzing this model, we have found that when the length of the time series exceeds some critical length, the DFA and MSE measurements from the time series remain relatively constant, and, in addition, they do not depend on initial conditions. This confirms that the statistics computed from the time series reflect properties of the underlying system, rather than the particulars of the measurement process.

In addition, we have made two important observations. Firstly, given a neural network $\mathcal{N}$ and simulations of various lengths, the intrinsic complexity of the signal is maintained over a wide range of time series lengths. This is key for computations involving optimization of network topology and parameter sets. It allows us to run large batches of simulations, each for a relatively short amount of time, confident that physiological complexity seen in the resulting time series coincides with that of a longer series.

Secondly, there exists a finite range of time scales over which the network displays complex behavior. This shows that the network $\mathcal{N}$ has a distinct limit to its capacity for complexity and is incapable of producing complexity at every time scale. This result serves to clarify the boundaries of an *in-silico* neural network's complex behavior. Thus, we can determine the upper bound of complexity inherent to each network and optimize with respect to this measurement as well. Future work will focus on expanding this boundary by optimizing over network size and coupling strengths.

The ultimate test of our model, however, is its ability to match concrete experimental physiological data. We are currently collaborating with a group that has access to clinical data for both healthy and ill individuals to see whether our model can simulate the statistics of physiological measurements obtained from both of these groups.

ACKNOWLEDGEMENTS

This research was partially supported by DARPA (JB, TG and KM), NSF grant DMS-0818785 (TG), NSF grants DMS-0511115 and 0835621 (KM) and the U.S. Department of Energy (KM).

REFERENCES

Costa, M., Goldberger, A. L., and Peng, C.-K. (2002). Multiscale entropy analysis of complex physiologic time series. *Phys. Rev. Lett.*, 89(6):068102.

Costa, M., Goldberger, A. L., and Peng, C.-K. (2005). Multiscale entropy analysis of biological signals. *Phys. Rev. E*, 71(2):021906.

Goldberger, A. L. (2006). Giles F. Filley Lecture. Complex Systems. *Proc Am Thorac Soc*, 3(6):467–471.

Goldberger, A. L., Amaral, L. A. N., Glass, L., Hausdorff, J. M., Ivanov, P. C., Mark, R. G., Mietus, J. E., Moody, G. B., Peng, C.-K., and Stanley, H. E. (2000). Physiobank, Physiotoolkit, and Physionet : Components of a New Research Resource for Complex Physiologic Signals. *Circulation*, 101(23):e215–220.

Katok, A. and Hasselblatt, B. (1997). *Introduction to the Modern Theory of Dynamical Systems*. Cambridge University Press.

Peng, C.-K., Buldyrev, S. V., Havlin, S., Simons, M., Stanley, H. E., and Goldberger, A. L. (1994). Mosaic organization of DNA nucleotides. *Phys. Rev. E*, 49(2):1685–1689.

Peng, C.-K., Havlin, S., Stanley, H. E., and Goldberger, A. L. (1995). Quantification of scaling exponents and crossover phenomena in nonstationary heartbeat time series. *Chaos: An Interdisciplinary Journal of Nonlinear Science*, 5(1):82–87.

Peng, C.-K., Yang, A. C.-C., and Goldberger, A. L. (2007). Statistical physics approach to categorize biologic signals: From heart rate dynamics to DNA sequences. *Chaos: An Interdisciplinary Journal of Nonlinear Science*, 17(1):015115.

Richman, J. S. and Moorman, J. R. (2000). Physiological time-series analysis using approximate entropy and sample entropy. *Am J Physiol Heart Circ Physiol*, 278(6):H2039–2049.

Terman, D., Ahn, S., Wang, X., and Just, W. (2008). Reducing neuronal networks to discrete dynamics. *Physica D: Nonlinear Phenomena*, 237(3):324–338.

APPENDIX

The network $\mathcal{N}$ used in Section 4 is generated by the 10-cell graph in Figure 1 with the parameter set P listed in the following tables.

Table 1: Parameter set for neural network $\mathcal{N}$, excluding ε's.

α	α_I	α_x	β	β_I	β_x	g_{EI}	g_{IE}	g_{II}
4.0	4.0	1.0	0.1	0.1	4.0	0.4	0.4	0.4
v_I	v_E	θ	θ_I	θ_x	b	c	K_I	K_E
3.0	0.1	0.1	0.1	0.1	0.8	0.7	0.28	0.35

Table 2: ε set for $\mathcal{N}$.

Excitatory	ε_1	0.08456607
	ε_2	0.00043158
	ε_3	0.00068327
	ε_4	0.06293498
	ε_5	0.00537958
Inhibitory	ε_1	0.00017724
	ε_2	0.03678080
	ε_3	0.05379177
	ε_4	0.00140943
	ε_5	0.00037465